MOLECULAR DYNAMICS SIMULATIONS OF THE DIFFUSION OF Li CATIONS IN LITHIUM FLUORHECTORITE CLAY MODELS.

SIMULACIONES DE DINÁMICA MOLECULAR DE LA DIFUSION DE CATIONES Li EN MODELOS DE LA ARCILLA LITIO FLUORHECTORITA.

A. Lam [a†], G. Rojas-Lorenzo[b]

a) Zeolite Engineering Laboratory, Institute of Material Science and Technology (IMRE), University of Havana, Havana, CP. 10400. Cuba; anabel@imre.uh.cu†
b) Instituto Superior de Tecnologías y Ciencias Aplicadas, Universidad de La Habana, Ave. Salvador Allende y Luaces, Quinta de Los Molinos, Plaza, La Habana 10600. Cuba.
† corresponding author

Recibido 25/12/2023; Aceptado 19/1/2024

We study, using the Molecular Dynamics method, the mobility of Lithium compensation cations in two clay models that are in contact with a water reservoir. The preferential site of Li^+ is the center of the hexagonal ring of the structure. The simulations show that Li^+ cations can leave their initial positions and move in four different ways. These movements occur over short time intervals, suggesting a jump diffusion mechanism. Furthermore, our simulations have highlighted that Li^+ can coordinate with the framework oxygens and with water molecules, and the solvation will depend on the position of the cation. Likewise, the cations close to the surface are the ones that diffuse the most.

Estudiamos, usando el método de Dinámica Molecular, la movilidad de los cationes de compensación Litio en dos modelos de arcilla que se encuentran en contacto con un reservorio de agua. El sitio preferencial del Li^+ es el centro del anillo hexagonal de la estructura. Las simulaciones muestran que los cationes Li^+ pueden abandonar sus posiciones iniciales y desplazarse de cuatro formas diferentes. Estos movimientos son en intervalos de tiempo cortos, lo que sugiere un mecanismo de difusión por saltos. Además, nuestras simulaciones han puesto de relieve que el Li^+ puede coordinar con los oxígenos del enrejado y con las moléculas de agua, y el grado de solvatación dependerá de la posición del catión. Así mismo, los cationes cercanos a la superficie son los que más difunden.

PACS: Molecular Dynamics Calculations (Cálculos de Dinámica Molecular) 31.15.xv, Diffusion in nanoscale solids (Difusión en sólidos en la nanoescala), 66.30.Pa, Computer modeling and simulation (Modelación y simulación computacional), 07.05.Tp.

I. INTRODUCTION

Clay minerals are a ubiquitous and important component of soils and sediments, and their properties are strongly influenced by their ability to exchange ions with their surroundings. The ion exchange capacity of clays is determined by the negative charge on their surfaces, which arises from the substitution of atoms in their crystal structure [1] for others with smaller valence. This charge can be neutralized by compensating cations, mainly Na^+, K^+, Ca^{2+}, Mg^{2+} and H^+ [2]. Diffusion of the water and cations in the interlayer spaces controls a large number of process like swelling and ion exchange. The exchange of ions between clays and their environment has significant implications for a range of processes, including nutrient cycling, soil fertility, and the transport of contaminants [3]. Also, the ion exchange capacity of clays has made them valuable in a wide range of industrial applications: production of detergents, water treatment, catalysis, and fabrication of ceramics, among others [4]. Understanding the mechanisms and rates of ion exchange in clays is therefore critical for predicting and managing the behavior of these important geological materials [1].

Computational simulation studies are an important tool in understanding the mechanism of cationic movement and ion exchange in clays. Molecular Dynamics simulations have been used to investigate the diffusive properties of cations in clays, revealing the role of the clay structure and surface charge on cationic movement [5–7]. Lithium fluorhectorite ($Li-Fh$) is a smectite clay that has been studied as a potential drug support [8–11]. This material has the property to increases its interlayer space with temperature. The $Li-Fh$ can incorporate up to three layers of water when the d-spacing is bigger than 17 Å [12,13]. Our research group has evaluated the interaction of $*Li-Fh$ with water and with ciprofloxacin, and in both studies, we were able to observe the mobility of the compensating cations [13,14]. It is well known that in these materials, the cations and the water molecules have freedom of movement. Li^+ is a small cation mainly located in the hexagonal cavity of the tetrahedral clay layer, and even as the hydration of the material increases, it remains very close to the lattice, unlike other cations such as sodium, which moves to the center of the interlayer space [12,13].

Considering that the movement of compensation cations is the first step in processes as ion exchange and swelling, that take place within very short periods, we have decided to use computational simulations as a tool to understand these complex processes. In particular, we have conducted Molecular Dynamics simulations of two clay models reproducing the 010 and 001 surfaces of the $Li-Fh$, in contact with a water reservoir. The 010 model has been used previously to reproduce the incorporation of molecules into the interlayer spaces [13]. The 001 model of $Li-Fh$ is used for the first time and will allow us to reproduce the processes on that surface. In both models, we aim at evaluating the mobility

of the Lithium cations and the interactions established with the lattice and water molecules. The results obtained here shed light on the nature of the interactions in order to understand the complex processes associated with the movement of cations in clays.

II. METHODOLOGY

As in our previous work [13, 14], the clay model used is a supercell of a $5 \times 5 \times 3$ unit cells of lithium fluorhectorite, which contains 900 water molecules in the interlayer spaces and was built as described in reference [13]. To simulate Li^+ motion on different clay surfaces, two different models were used. In the first model, see Figure 1a, the periodicity in the 010 direction was cleaved and a slab of 30 Angstroms with 1493 water molecules was inserted in the simulation box. This model was previously used to simulate the interaction of the clay model with the outer water solution [14]. The valences of *Si* and *O* atoms on the surface were compensated by adding *OH* and *H*, respectively, and ending the tetrahedral clay edges with *OH* groups. Meanwhile, octahedral ions (Mg^{2+}, Li^+, and F^-) were not balanced. In the second model, the periodicity in the 001 direction was cleaved and a slab of 30 Angstroms with 1205 water molecules was inserted, see Figure 1b. In this model, it was not necessary to compensate the valences. The water density in the slab of both models was around 1 g/cm^3.

CLAYFF was the force field used to describe the interaction of clay [15]. Further details on the potential used for the OH valence compensating groups in the 010 clay model can be found in Reference [14]. The parameters for the Li^+ compensating cation were taken from Koneshan et al. [16].

All MD simulations were performed using DL_POLY software [17]. Different simulation strategies were performed to equilibrate the systems. For the 010 model, the clay framework and water were first fixed, and only the clay terminal OH was allowed to relax during a 1 ps in the NVE ensemble with a time step of 10^{-16} s at 300 K. Then, the water and *OH* terminal were relaxed while keeping the clay framework fixed in the NVT ensemble during 2 ps at 300 K with a time step of $5{\times}10^{-16}$ s. After that, all atoms were relaxed, except for those *Li* and *F* in the octahedral sheets that are in contact with the water solution. These atoms were fixed during the simulations to avoid possible diffusion, and a simulation in NPT ensemble of 100 ps at 300 K, 1 atm, and a time step of 1 fs was performed.

For the 001 model, a one-step strategy was followed to equilibrate the system: a simulation during 1 ps in the NVT ensemble at 300 K, in which the first 0.5 ps were performed with temperature control, and with an integration step of 10^{-16} s.

Once both models (010 and 001) were perfectly equilibrated, the production runs of 20 ns were performed in the NPT ensemble at a temperature of 300 K, pressure of 1 atm, and 1 fs integration step. The Nosé-Hoover thermostat and barostat were used, each with a 100 fs relaxation time, respectively. In all simulations, periodic boundary conditions were applied. The Ewald summation method was used to calculate the electrostatic interactions of the systems and the cutoff of the long-range interactions, the Coulomb and the Lennard-Jones potentials, were set to 10 Angstroms. The trajectory of the atoms in the NPT simulations was collected every 5000 steps for dynamics and structural analysis.

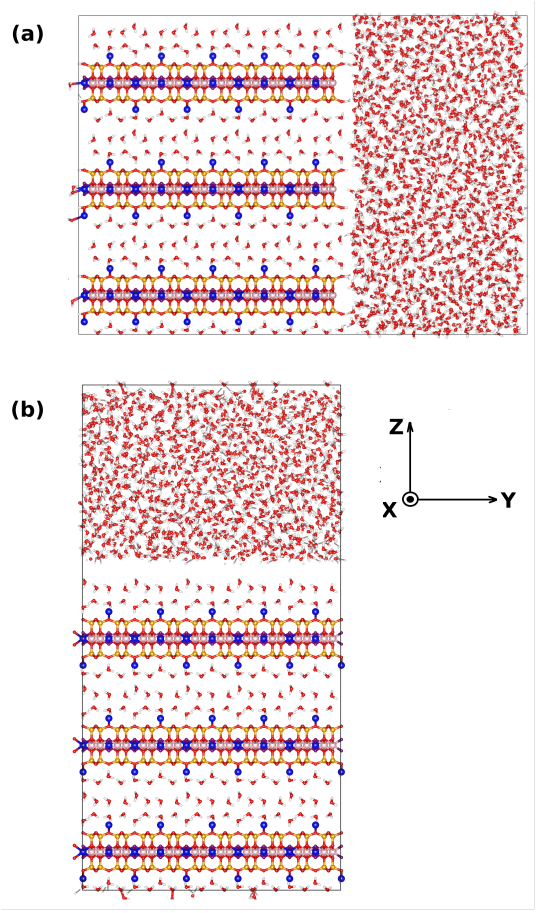

Figure 1. The models used in the simulation, (a) 010 Model, (b) 001 Model. The orange, red, blue, pink, violet, and white balls correspond to *Si*, *O*, *Li*, *Mg*, *F*, and *H* atoms, respectively. The simulation boxes are delimited by the black rectangles.

III. RESULTS

III.1. Diffusion at 010 surface

In the 010 model, there are a total of 150 Li^+ compensating cations, with 30 located at each edge and the remaining 90 distributed within the clay. It is presumed that these 90 cations are situated in the bulk of the clay. Li^+, being a small cation, is typically found in the center of the hexagonal ring of the framework, where it coordinates with the oxygen atoms of the framework and water molecules [13]. In clays, Li^+ ions have the ability to diffuse within the interlayer or migrate to the outer water solution. Upon diffusion, Li^+ ions may return to their original positions or occupy new positions. It is more likely that the Li^+ ions located at the edges will diffuse towards the outer solution, as they are located at the boundary.

In the simulation of the 010 model, 20 Li^+ move from their original positions, of which 19 are edge Li^+ and only one belongs to the inner layer, moving to the interlayer spaces. Li^+

can move from their original positions and diffuse in different pathways, some of which are:

I. Cross the interlayer.

II. Jump to another hexagonal ring of the same layer.

III. Diffuse into the solution or in the interlayer.

IV. Move to the octahedral edge.

In some cases, the same Li^+ could combine some of the previously described motions. Some examples of these possibilities are shown in Figure 2, which presents a snapshot at 6 ns of the simulation. As can be observed, some Li^+ cations have moved from their original positions. In the figure, the displacement prior to 6 ns is represented using numbers associated with the previously mentioned motions. It can be noted that one Li^+ cation (labeled as 2733), moves in the interlayer, occupies a different hexagonal ring from its starting position, and diffuses into the solution. This cation crosses the solution and finally settles in a hexagonal ring on the opposite edge of the clay model.

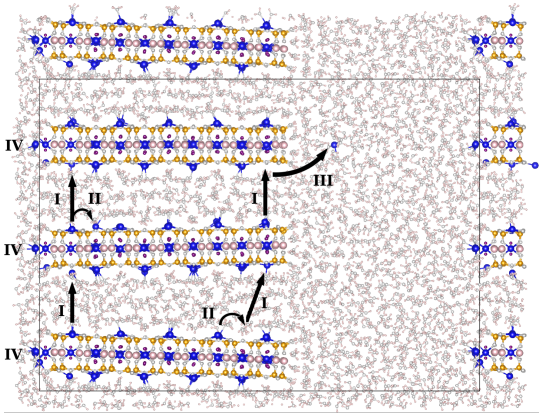

Figure 2. Snapshot at $6,595$ ns of the simulation. Various movements of the Li^+ cations in the 010 model are depicted and denoted using Greek numbers as explained in the text. The simulation box is indicated within the black rectangle, and boundary conditions were applied to enhance visualization. Si, Mg, F, and Li are represented by orange, pink, violet, and blue spheres, respectively. Additionally, O and H are depicted in white to further aid visualization.

Figure 3 shows the displacements of the cations observed during the simulations. In Figure 3a, the cations that cross the interlayer (mechanism I) are depicted. With the exception of the Li^+ labeled as 2173, which returns to the original layer, the remaining cations are accommodated in a hexagonal cage within the opposite layer. These cations cover distances ranging from 10.24 to 17.48 Angstroms.

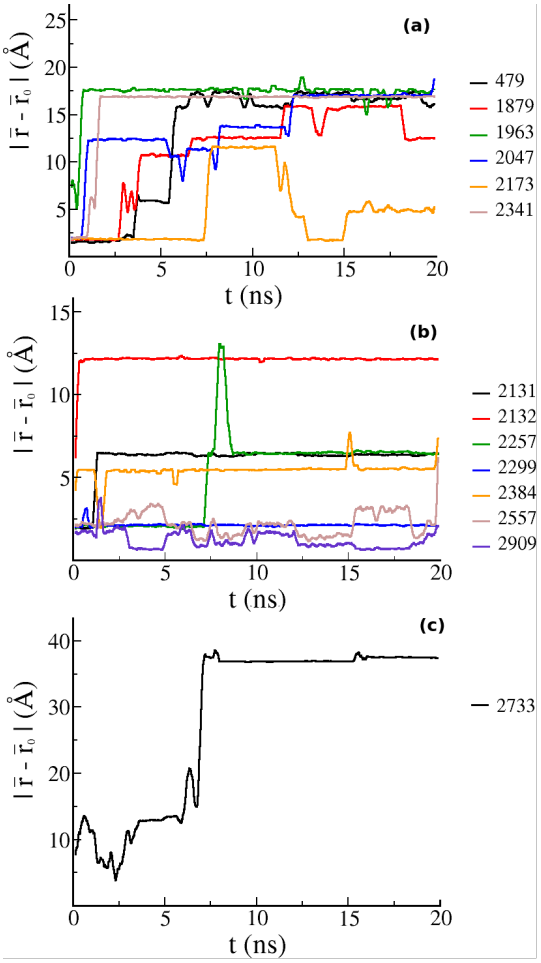

Figure 3. Displacement of the Li^+ cations that diffuse during the simulation in 010 model. They have been divided into three different groups: (a) Li^+ that cross the interlayer, (b) Li^+ that jump to the another hexagonal ring in the same layer and (c) the Li^+ that shows all the possible motions.

Figure 3b illustrates the Li^+ ions moving within the same layer from their original position, following mechanism II, by jumping to another hexagonal cage. The distance between adjacent hexagonal cages is around 5-6 Å. Additionally, Figure 3c showcases the displacement of the Li^+ labeled as 2733, which, as previously explained, diffuses to different hexagonal cages and also into the solution. As depicted in Figure 3, the time that Li^+ ions transition to new positions is brief, suggesting rapid motions. They swiftly move from one position to another, where they remain for longer durations and these correspond to the plateaus of Figure 3. This type of diffusion mechanism closely resembles jump diffusion, which entails sequences of site-to-site jumps. A similar mechanism has been previously documented in the diffusion of water in clays and hydrocarbons in zeolites [18–20].

III.2. Diffusion at 001 *surface*

In the model 001 there are also 150 Li^+ compensating cations, 50 of them in contact with the water reservoir and the remaining 100 placed in the interlayer spaces. Only the cations

in contact with the water reservoir can diffuse towards the outer solution. The one hundred Li^+ ions in the interlaminar spaces, due to periodic boundary conditions, behave as if they were in the bulk of an infinite crystal and do not interact with the water reservoir. For model 010, we defined four diffusion pathways for the Li^+ in contact with the water reservoir. In certain cases, some cations may exhibit a combination of the above mentioned pathways. However, in model 001, mechanism IV is excluded because the model lacks of an exposed octahedral edge on the surface.

At the beginning of the simulation, at least 7 cations were out of position in the hexagonal rings of the clay structure. At 190 fs, five Li^+ returned to the hexagonal cages, with three of them occupying positions different from their starting one. Between 925 fs and 2.45 ns, the Li^+ labeled as 560 diffuses throughout the water reservoir, returning to the same starting clay layer but occupying a different hexagonal cage located at the border of the simulation box. From 3.745*n*s to 7.1 ns, the Li^+ labeled as 880, diffuses through the water reservoir and finally settles into a different hexagonal cage.

Diffusion pathway III is associated with significant displacements in the water reservoir. At least 2 Li^+ diffuse throughout the solution during the simulation, labeled as 560 and 880. Figure 5 illustrates different snapshots of the simulation where those cations are in the solution. The black and blue curves of Figure 4 correspond to Li^+ cations 560 and 880, respectively, and show that those cations diffuse nearly 40 Å. Around the 15.5 ns, the Li^+ labelled as 39 (line maroon in Figure 4) jumps to the neighboring hexagonal cage. After 15.8 ns, no further Li^+ diffusion was observed, and the cations then move in tandem with the clay structure, vibrating around their equilibrium positions.

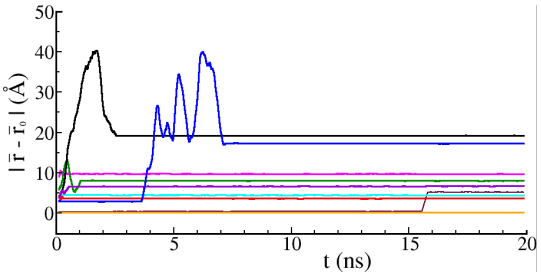

Figure 4. Displacement of the Li^+ that diffuse during the simulation in 001 model.

As depicted in Figure 4, the duration of the diffusion process is relatively short compared to the time that the species remain in the same position, indicating a jump mechanism diffusion, as was observed in model 010, and previously reported for the diffusion of guest molecules in porous and layered materials [18–20].

Table 1 shows the Diffusion coefficients (D) of the Li^+ and water molecules in the two clay models. The D values are very similar in both models. However, the lithium cations diffuse more in the 001 model, probably because in this model two Li^+ diffuse to the outer solution, instead of one in the 010 model. The values are also similar to those reported in reference 14. Furthermore, the water diffusion coefficient is higher in the 010 model because in this model the water of the interlayer can diffuse to the water reservoir and viceversa.

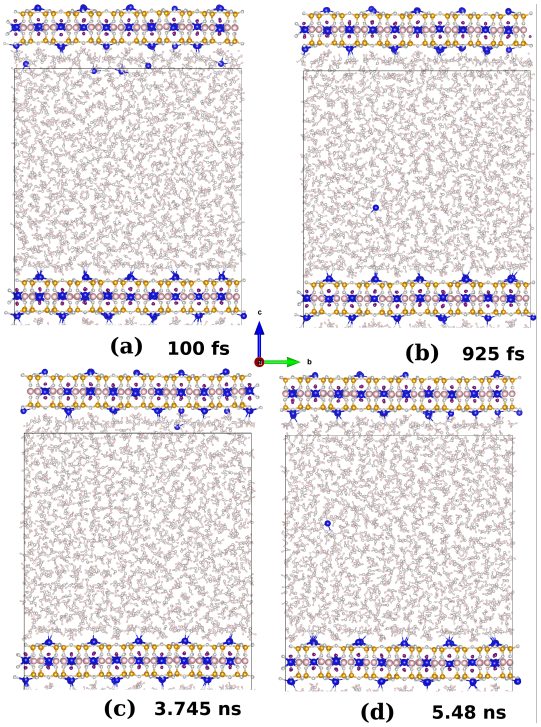

Figure 5. Snapshots of different stages during the simulation in the 001 model: (a) 100 fs, (b) 925 fs, (c) 3.745 ns, and (d) 5.48 ns. In Figure (b), the Li^+ labeled as 560 diffuses through the water reservoir, while in Figures (c) and (d), the Li^+ labeled as 880 diffuses through outer solution. Oxygen and hydrogen atoms are depicted in white to highlight the Li^+, while silicon, magnesium, fluorine, and lithium are represented by orange, pink, violet, and blue, respectively.

Table 1. Diffusion coefficients (D) of the Li^+ and water molecules in the clay models.

	D ($\times 10^{-9}$ m^2 s^{-1})	D ($\times 10^{-9}$ m^2 s^{-1})
Model	010	001
Li^+	1.2427×10^{-3}	6.3917×10^{-3}
OW	4.1367	3.0629
HW	4.1384	3.0636

III.3. Coordination of Li^+

As discussed in our previous publication [13], quantum calculations and MD simulations have demonstrated that Li^+ cations are typically found at distances ranging from approximately 2.14 to 2.5 Å from the oxygen atoms within the hexagonal cage. Our quantum calculations in the ciprofloxacin-LiFh model revealed that the drug was successfully intercalated in the interlayer, prompting the Li^+ cation to penetrate the clay layer, while the interaction with water was not simulated.

Li^+ cations can coordinate with the oxygen atoms of the clay, specifically those within the tetrahedral sheet (labeled as O), while omitting those in contact with the octahedral sheet. Additionally, Li^+ cations can also coordinate with the oxygen atoms of water molecules (OW).

Figure 6 illustrates the radial distribution function of the $O - Li^+$ and $Li^+ - OW$ pairs for both simulated models. The function appears notably similar in both models, with the first peak occurring within the range 2.1 – 3.3 Angstroms and reaching its maximum at 2.5 Å.

Furthermore, Figure 7 depicts the $n(r)$ values of $O - Li^+$ and $Li^+ - OW$ at 3.3 Å. Here, $n(r)$ represents the average number of type"b" atoms within a sphere of radius r around an atom of type "a".

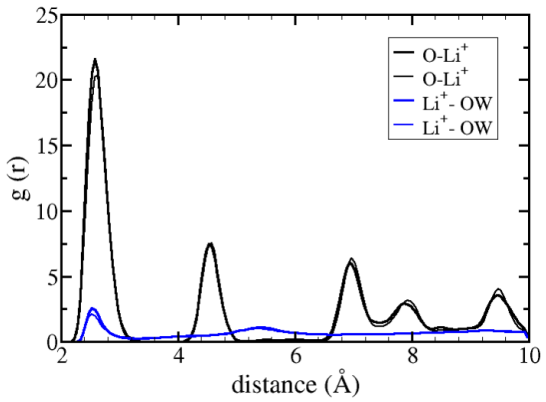

Figure 6. Radial distribution function of the pairs Oclay-Li^+ ($O - Li^+$) and Owater-Li^+ (Li^+-OW) of both simulated models. The thick lines belong to the 010 model and the thin lines to the 001 model.

The $n(r)$ value for the $O - Li^+$ pair is 0.92 and 0.997 in the 010 and 001 models, respectively, closely approximating 1. This suggests that each O atom has one Li^+ placed at a distance lower than 3.3 Å. These findings strongly suggest that Li^+ cations are positioned at equidistant locations from the O, possibly at the center of the hexagonal cage, as previously noted by us [13]. Conversely, the $n(r)$ values for the Li^+-OW at a distance of 3.3 Åare 1.7 and 1.5 in the 010 and 001 models, respectively, indicating the average number of water molecules coordinated by each Li^+. As depicted in Figure 8a, the Li^+ cations within the hexagonal cage can coordinate with the six O atoms as well as one OW atom.

Figure 8 a shows the interaction of one Li^+ with the six oxygen atoms of the hexagonal cage and one water molecule. Figure 8b shows the hydration sphere of one of the Li^+ that is not coordinated with the O clay, but is close to the layer. This Li^+ has six OW at distances lower than 2.8 Å, two of them at 2.5 Å.

However, those Li^+ ions that are not in close proximity to the layer coordinate a greater number of water molecules, as evident in Figure 8b. This type of Li^+ exhibits six OW atoms at distances of less than 2.8 Å, two of which are at 2.5 Å. These facts suggest that the $n(r)$ of the $Li^+ - OW$ is an average of all possible coordinations that water can establish with the cation.

In previous work, quantum calculations have suggested that Li^+ coordinate four water molecules within their first hydration sphere, with $Li^+ - OW$ distances lower than 1.876 Å. When the number of water molecules in the hydration sphere increases to six, the $Li^+ - OW$ distance extends to around 1.9 Å [21]. Additionally, [22] reports $Li^+ - OW$ distances of 2.150 Åfor $Li(H_2O)_6$ cluster.

However, quantum simulations are restricted in terms of the number of water molecules in the system, typically modeling a cluster with a limited number of molecules. It's notable that the $Li^+ - O$ distance increases with the increasing number of water molecules.

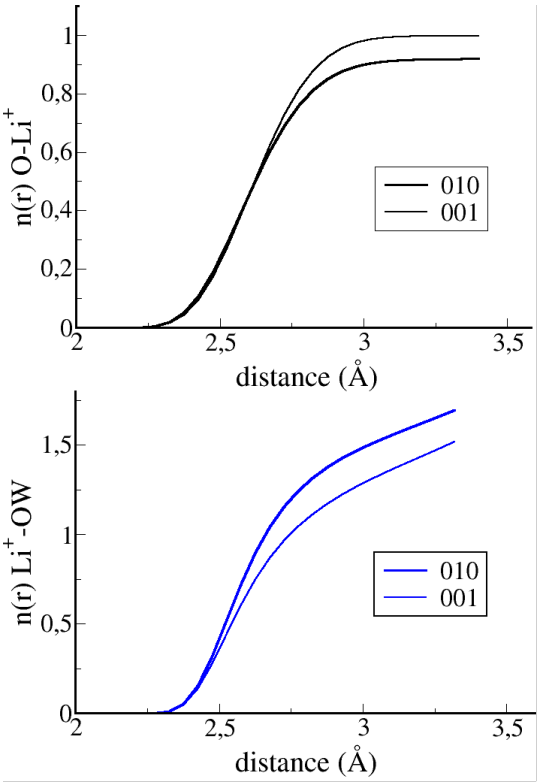

Figure 7. $n(r)$ $O - Li^+$ and $n(r)$ $Li^+ - OW$ of both simulated models. The thick lines belong to the 010 model and the thin lines to the 001 model.

More recent findings by Adapa and Malani [23] have reported a $Li^+ - O$ coordination value of 1 and for $Li^+ - OW$ and of 3 for mica, indicating a significant difference from the observations

for the sodium cations in these materials.

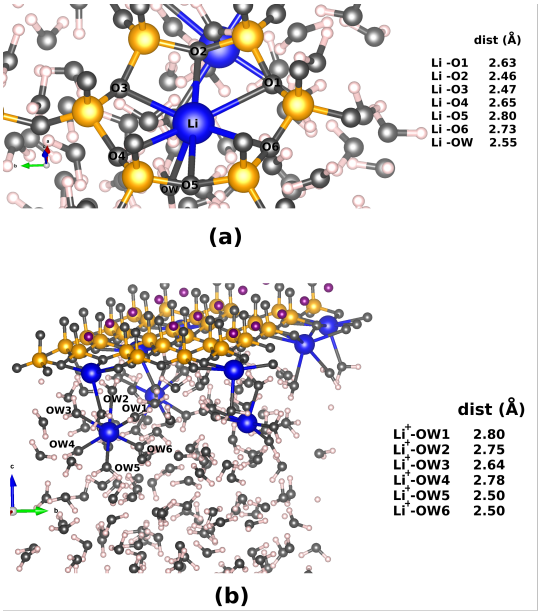

Figure 8. Different snapshots of the coordination of Li^+ with O and OW.

IV. CONCLUSION

Two models, the 010 and 001, have been used to study the diffusion process of the Lithium cations in the $Li-Fh$ clay using Molecular Dynamics simulations. They reveal that the Li^+ can move from their original position in the clay framework and exhibit different diffusion motions: it can cross the interlayer, move to another hexagonal ring of the same layer, diffuse in the interlayer or to the outer water solution, or move and accommodate at the octahedral edge.

The analysis of the radial distribution functions has confirmed that the preferred site for the Li^+ is positioned at the center of the hexagonal ring in the clay framework. Additionally, our observations have highlighted the capacity of Li^+ to coordinate with water molecules, where the extent of water solvation is contingent upon the cation's position.

Diffusion coefficients of Li^+ and water are very similar in both models, and the values indicate that Li^+ diffuses more stringly in the 001 model. Notably, our findings indicate that surface-close Li^+ cations exhibit a higher degree of mobility when compared to those within the bulk.

ACKNOWLEDGMENTS

A. L. and G. R-L. would like to thank Cuban National Programs PN211LH008-027 and PN223LH010-017 for financial support

REFERENCES

[1] G. Sposito. The Chemistry of Soils. Oxford University Press. (1989).

[2] M.F. Brigatti, E. Galan and B.K.G. Theng, "Structure and Mineralogy of Clay Minerals"Developments in Clay Science, Vol. 5, pp. 21-81. Elsevier. (2013).

[3] S. Guggenheim, R.T. Martin. Clays Clay Miner. **43**, 255 (1995).

[4] F. Bergaya, B.K.G. Theng and G. Lagaly. Handbook of Clay Science. Elsevier. (2006).

[5] J. Greathouse, R. Cygan, J. Fredrich and G. Jerauld. J. Phys. Chem. C. **120**, (2016).

[6] T. Underwood, V. Erastova, H.C. Greenwell. Clays Clay Miner. **64**, 472 (2016).

[7] T.A. Ho, L.J. Criscenti and J.A. Greathouse. J. Phys. Chem. Lett. **10**, 3704 (2019).

[8] A. Rivera, L. Valdés, J. Jiménez, I. Pérez, A. Lam, E. Altshuler, L.C. de Ménorval, J.O. Fossum, E.L. Hansen, Z. Rozynek. Appl. Clay Sci. **124-125**, 150 (2016).

[9] L. Valdés, D. Hernández, L.C. de Ménorval, I. Pérez, E. Altshuler, J.O. Fossum and A. Rivera. Eur. Phys. J. Spec. Top. **225**, 767 (2016).

[10] L. Valdés, S.A. Martín, D. Hernández, L. Lazo, L.C. de Ménorval, A. Rivera. Rev. Cubana Fis. 34, **35** (2017).

[11] D. Hernández, L. Lazo, L. Valdés, L.C. de Ménorval, Z. Rozynek, A. Rivera. Appl. Clay Sci. **161**, 395 (2018).

[12] T.J. Tambach, P.G. Bolhuis, E.J.M. Hensen and B. Smit. Langmuir **22**, 1223 (2006).

[13] A. Lam, G. Rojas-Lorenzo, A. M. Ferrari, A. Rivera, C.M. Zicovich-Wilson and L.J. Alvarez. Rev. Cubana Fis. **37**, 34 (2020).

[14] [14]A. Lam and G. Rojas-Lorenzo. Rev. Cubana Fis. **39**, 85 (2022).

[15] R.T. Cygan, J.-J. Liang and A.G. Kalinichev. J. Phys. Chem. B **108**, 1255 (2004).

[16] S. Koneshan, J.C. Rasaiah, R.M. Lynden-Bell and S.H. Lee. J. Phys. Chem. B **102**, 4193 (1998).

[17] I. Todorov, W. Smith, K. Trachenko and M. Dove. J. Mater. Chem. **16**, 1911 (2006).

[18] H. Jobic. Microporous Mesoporous Mater. **55**, 159 (2002).

[19] R.R. Desai, V.K. Sharma, S. Prabhudesai, S. Mitra, J. Desa, R. Mukhopadhyay. J. Phys. Soc. Japan. **82**, SA008 (2013).

[20] S. Mitra, V.K. Sharma and R. Mukhopadhyay. Rep. Prog. Phys. **84**, 066501 (2021).

[21] E.A. Gomaa, M.A. Tahoon, A. Negm. J. Mol. Liq. **241**, 595 (2017).

[22] D. Spångberg and K. Hermansson. J. Chem. Phys. **120**, 4829 (2004).

[23] S. Adapa, A. Malani. Sci. Rep. **12**, 17810 (2022).